Carbohydrate Polymers 112 (2014) 245–254

Contents lists available at ScienceDirect

Carbohydrate Polymers

journal homepage: www.elsevier.com/locate/carbpol

Characterization of an amylose-*graft*-poly(n-butyl methacrylate) copolymer obtained by click chemistry by EPR and SS-NMR spectroscopies

Silvia Borsacchi[a,b], Lucia Calucci[c], Marco Geppi[a,b], Federico La Terra[a], Calogero Pinzino[c], Monica Bertoldo[d,*]

[a] *Dipartimento di Chimica e Chimica Industriale, Università di Pisa, Via Risorgimento 35, 56126 Pisa, Italy*
[b] *INSTM, Consorzio Interuniversitario per la Scienza e Tecnologia dei Materiali, via Giusti 9, 50121 Firenze, Italy*
[c] *Istituto di Chimica dei Composti Organometallici del Consiglio Nazionale delle Ricerche, Area della Ricerca di Pisa-S. Cataldo, Via G. Moruzzi 1, 56124 Pisa, Italy*
[d] *Istituto per i Processi Chimico-Fisici del Consiglio Nazionale delle Ricerche, Area della Ricerca di Pisa-S. Cataldo, Via G. Moruzzi 1, 56124 Pisa, Italy*

ARTICLE INFO

Article history:
Received 6 March 2014
Received in revised form 28 April 2014
Accepted 19 May 2014
Available online 6 June 2014

Keywords:
Amylose
Click chemistry
Graft copolymers
MAS NMR
PBMA
Nuclear relaxation times

ABSTRACT

We present an investigation of the main chemical and physico-chemical properties of a graft copolymer of amylose and poly(n-butyl methacrylate), Am-g-PBMA, amphiphilic and able to self-assemble in water, prepared by coupling end azide-functionalized PBMA and alkyne-functionalized amylose under convenient click conditions. A deep knowledge of these properties is necessary in the perspective of real applications of the copolymer. To this aim we combined a basic characterization through FT-IR, TGA, ICP-OES and SEM with an extensive EPR and Solid State NMR investigation. It was possible to characterize the main structural and dynamic properties of Am-g-PBMA and highlight the presence of residual copper (Cu(II)) from the catalyst, even after an extensive purification procedure. We could identify two main species of Cu(II): Cu(II) complexes coordinated to the *N*,*N*,*N*′,*N*″,*N*″-pentamethyldiethylenetriamine (PMDETA) ligand from the catalyst and to the copolymer triazole nitrogens and multi-nuclear or clustered Cu(II) species likely coordinated to amylose hydroxyl groups.

1. Introduction

Graft copolymers based on polysaccharides have received much attention for their possible multiple applications (Kalia & Sabaa, 2013). In particular, they can be used as flocculants (Singh, Pal, Krishnamoorthy, Adhikary, & Ali, 2009), as adsorbents in wastewater treatment (Adhikary & Krishnamoorthi, 2012; Crini, 2005; Xu, Zhang, & Feng, 2013; Zhang et al., 2014), for oil recovery (Karmakar & Singh, 1997), and as drag reducing agents (Singh et al., 2000, 2009). They have been investigated also as possible compatibilisers in biodegradable blends and composites of starch and cellulosic materials (Ciardelli & Penczek, 2004; Mooney, 2009; Nafchi, Moradpour, Saeidi, & Alias, 2013; Shogren et al., 1992).

From a structural point of view, polysaccharide graft copolymers are usually composed by a polysaccharide backbone and by synthetic grafted chains. They typically combine the properties of the two components but they have also new properties (Hadjichristidis, Pispas, Pitsikalis, Iatrou, & Lohse, 2004) such as the ability to self-assemble into nanostructured morphologies (Beiner & Huth, 2003; Feng et al., 2011). In addition, they can stabilize multiphase materials (Ciardelli & Penczek, 2004). In particular, graft copolymers of polysaccharides with hydrophobic polymers are amphiphilic and can thus self-assemble in water into spherical nanoparticles (Bertoldo, Zampano, La Terra, Villari, & Castelvetro, 2011; Feng et al., 2011) or in more complex nanostructures, which can be used as templates to grow nanostructured inorganic materials, as photonic gratings (Feng et al., 2011), or as drug delivery particles (Liu, Jiao, Wang, Zhou, & Zhang, 2008; Maiti, Ranjit, & Sa, 2010). For instance, particles made of amylose graft copolymers can be used for colon-specific delivery due to the resistance of this polysaccharide to the acidic environment (Alias, Goñi, & Gurruchaga, 2007; Silva, Gurruchaga, & Goñi, 2009).

* Corresponding author. Tel.: +39 050 315 2250; fax: +39 050 315 2230.
E-mail addresses: silvi@dcci.unipi.it (S. Borsacchi), lucia.calucci@pi.iccom.cnr.it (L. Calucci), marco.geppi@unipi.it (M. Geppi), federicolt@libero.it (F. La Terra), calogero.pinzino@pi.iccom.cnr.it (C. Pinzino), monica.bertoldo@ipcf.cnr.it (M. Bertoldo).

http://dx.doi.org/10.1016/j.carbpol.2014.05.086
0144-8617/

From a physical point of view, graft copolymers have properties that differ from those of the corresponding constituents and blends because of the different chain arrangement and dynamics. Properties typically affected are the glass transition temperature, the melting point, and the crystallinity degree (Mataz & Gregory, 2005).

Graft copolymers have been prepared combining preformed polymers by suitable coupling reactions, or by grafting using anionic, radical, or controlled radical polymerization methods (Feng et al., 2011; Hadjichristidis et al., 2004; Matyjaszewski & Spanswick, 2005). Amylose based graft copolymers have been prepared mainly by radical polymerization initiated by Ce(IV) that acts as hydrogen abstractor on the polymer backbone (Goni, Gurruchaga, Valero, & Guzman, 1983; Goñi et al., 1994; Karmakar & Singh, 1997; Pascual, Castellano, Vazquez, Gurruchaga, & Goñi, 1996; Vazquez, Goni, Gurruchaga, Valero, & Guzman, 1987). These methods do not allow any control over the length and density of the grafted chains. On the other hand, a full control of these properties has been obtained by anionic polymerization from a polysaccharide preventively modified to protect the hydroxyl groups that had not to be grafted (Ouhib et al., 2009). A simpler and fully controlled synthetic method has been recently developed by some of us (Bertoldo et al., 2011) by combining atom transfer radical polymerization (ATRP) (Matyjaszewski & Xia, 2001) and the copper-catalyzed version of the Huisgen 1,3-dipolar cycloaddition reaction between terminal acetylenes and azides ("click reaction") (Rostovtsev, Green, Fokin, & Sharpless, 2002). This method revealed successful for the preparation of amylose grafted with poly(*n*-butyl acrylate), poly(*n*-butyl methacrylate), poly(*n*-hexyl methacrylate), and poly(N,N-dimethylaminoethyl methacrylate). Indeed, ATRP provides a simple route to many well-defined (co)polymers with predetermined molecular weight, narrow molecular weight distribution, and high degree and variety of chain-end functionalities (Matyjaszewski, Gnanou, & Leibler, 2007; Matyjaszewski & Tsarevsky, 2009; Matyjaszewski & Xia, 2001) including alkyne or azide (Bertoldo et al., 2011; Sumerlin, Tsarevsky, Louche, Lee, & Matyjaszewski, 2005; Vogt & Sumerlin, 2006). On the other hand, the click reaction is robust and highly selective also in the case of polymers with many functionalities, such as proteins and polysaccharides (Elchinger et al., 2011; Thirumurugan, Matosiuk, & Jozwiak, 2013). As a consequence, several groups used the click reaction to prepare polysaccharide grafted copolymers (Bertoldo et al., 2011; Kulbokaite, Ciuta, Netopilik, & Makuska, 2009; Nakagawa, Kamitakahara, & Takano, 2012; Peng et al., 2012; Uliniuc et al., 2013). However, it must be pointed out that this reaction has the draw-back of using copper as catalyst and copper is able to strongly coordinate to several end groups (Matyjaszewski, 2012; Wang et al., 2012).

In this paper, we investigated structural and dynamic properties of a graft copolymer of amylose, the linear polysaccharide formed by α-1,4-linked glucose units which constitutes 20–30% of starch structure (Stumpf, Conn, & Preiss, 1988), and poly(n-butyl methacrylate) (PBMA). The amylose-graft-poly(n-butyl methacrylate) copolymer, Am-g-PBMA, was prepared by coupling end azide-functionalized PBMA (PBMA-N3) and alkyne-functionalized amylose (Am-PA) under typical click conditions, according to a procedure reported by some of us (Bertoldo et al., 2011). Although a purification procedure, consisting in several dissolution–precipitation steps followed by extensive dialysis against water, was performed, residual copper from the catalyst was found in the copolymer by Inductively Coupled Plasma Optical Emission Spectrometry (ICP-OES) 0analysis. Given the reaction and purification conditions, we can estimate that the major part of Cu(I) introduced with the catalyst is oxidized to Cu(II), which has the potential to form stable complexes with nitrogen- and oxygen-containing ligands arising from the catalyst and/or the copolymer functional groups. In particular, Cu(II) has been found to give complexes with hydroxyl groups of amylose (Ciesielski & Tomasik, 2004; Li et al., 2013, 2014) and with 1,2,3-triazole groups (Zhang, Junk, Luo, Hinderberger, & Zhu, 2010). Since Cu(II) species are paramagnetic, Electron Paramagnetic Resonance (EPR) spectroscopy was applied in order to ascertain the environment of Cu(II) in our copolymer. Indeed, EPR spectroscopy is a powerful technique for characterizing the type of bonded atoms, the number of ligands and the structure of Cu(II) complexes and it has been successfully employed to investigate the coordination of Cu(II) in polymers containing triazole groups (Zhang et al., 2010) and in starchy substrates (Ciesielski & Tomasik, 2004; Łabanowska, Bidzińska, Dyrek, & Szymońska, 2006), as well as for a detailed analysis of the Cu(II) species forming during copper-mediated ATRP (Caretti, Dervaux, Du Prez, & Van Doorslaer, 2010). Moreover, to get insights into the structural and dynamic properties of the prepared grafted copolymer, a combination of ^{13}C high-resolution and ^{1}H low-resolution Solid State Nuclear Magnetic Resonance (SS-NMR) experiments was carried out and analyzed considering both the copolymer composition and the presence of paramagnetic Cu(II) species. In fact, SS-NMR is at present one of the most powerful techniques available to access structural and dynamic properties of solid complex materials on wide spatial (0.1–100 nm) and time (ps–s) scales, independently of their crystalline or amorphous nature (Geppi, Borsacchi, Mollica, & Veracini, 2009; Geppi, Mollica, Borsacchi, & Veracini, 2008).

2. Materials and methods

2.1. Materials

Amylose (type III) from potatoes, essentially free from amylopectin (<1% by ^{1}H NMR analysis), was purchased from Aldrich. Tetrahydrofuran (THF) was kept on NaOH for 24 h, then distilled (67 °C) under nitrogen atmosphere. Sodium borate buffer (1 M, pH 8.5) was obtained by basification of a boric acid solution. Butyl methacrylate (BMA) was distilled from CaH_2 under nitrogen atmosphere (57 °C, 18 mmHg). CuBr (Aldrich, 99.999%) was stored under nitrogen and used without further purification. 2-Bromo-isobutyric acid 3-azidopropylester (BIAA) was synthesized by following a previously reported procedure (Bertoldo et al., 2011). 1,1,4,7,10,10-hexamethyltriethylenetetramine (HMTETA, Sigma–Aldrich, 97%), *N*,*N*,*N*′,*N*″,*N*″-pentamethyldiethylenetriamine (PMDETA, Sigma–Aldrich, 99%), propargylamine (Sigma–Aldrich, 98%), sodium periodate (Aldrich, 99.8+%), sodium cianoborohydride (Aldrich, 95%), and all other solvents were used as received.

2.2. Synthesis of the amylose-graft-poly(n-butyl methacrylate) copolymer (Am-g-PBMA)

The synthesis of Am-g-PBMA (Scheme 1) was accomplished by following a previously reported strategy (Bertoldo et al., 2011); for a detailed description see Supplementary data.

2.3. Preparation of reference samples for EPR analysis

A 0.07 M solution of the CuBr/PMDETA catalyst in DMF was obtained from equimolar amounts of CuBr and PMDETA. The solution was mixed with amylose in DMSO (Cu/amylose 0.7 mmol/g) to obtain a catalyst/amylose mixture. Both samples were diluted with a 1:2 DMF/DMSO mixture before analysis.

PBMA-T was obtained by reacting PBMA-N3 (53 μmol of azide) and propargylamine (53 μmol) in DMSO/DMF 2/1 (6 ml) in the presence of CuBr/PMDETA (0.055 μmol) and 0.01 g of sodium ascorbate (Scheme 2). The reaction was carried out under nitrogen atmosphere for 24 h at 40 °C, and then cooled to room temperature. The

mixture was exposed to air and diluted with an oxygenated 1:2 DMSO/DMF mixture before analysis. The disappearing of the azide stretching band in the infrared spectra of the product (see Supplementary data) and the observation of the ^{1}H NMR signal at 7.60 ppm (300 MHz, $CDCl_3$, 25 °C) indicated the clicking between the terminal azide group of PBMA-N3 and propargylamine with formation of a triazole ring.

2.4. Characterization methods

Infrared spectra were recorded with a PerkinElmer Spectrum One FT-IR spectrophotometer interfaced with the software Spectrum v.3.02 for data acquisition. Samples were analyzed in transmission mode as cast films on KBr windows or prepared in KBr discs.

^{1}H NMR spectra in solution were recorded with a Varian 300 MHz instrument on $CDCl_3$ or DMSO-d_6, solutions. Sample concentration was ~30 mg/mL.

Elemental analyses (C, N, H) were performed on a Carlo Erba 1106 elemental analyzer.

Size exclusion chromatography (SEC) analyses were carried out with a Jasco instrumental setup consisting of a PU-2089 Plus high pressure pump, column oven, RI 2031 Plus (refractive index) and UV-2077 Plus (UV) detectors. The instrument was equipped with two PLgel 5 μm Mixed-D columns (Polymer Laboratories) kept at 40 °C and eluted with $CHCl_3$ (1 mL/min). Data were acquired and processed with the Borwin 1.21.61 (JMBS development) software. Sample concentration was in the 3–5 mg/mL range and injection volume was 20 μL. The instrument was calibrated with polystyrene standards.

Thermogravimetric analyses (TGA) were carried out with a Mettler Toledo TGA/SDTA 851e instrument under 60 mL/min nitrogen flux in the 25–700 °C temperature range at a 10 °C/min heating rate on 20–30 mg samples.

ICP-OES analyses were performed using a Varian 720 ES instrument. Samples were treated with 65% HNO_3 and 30% H_2O_2 and digested in a Milestone Start D microwave apparatus.

EPR spectra were recorded on a Varian (Palo Alto, CA, USA) E112 spectrometer operating at X band equipped with a Varian E257 temperature control unit. For each spectrum, a microwave power of 10 mW and a modulation amplitude of 1.25 G were employed. The spectra were fitted using the SIMPIP program (Nilges, 1998). The calculations were performed considering both ^{63}Cu and ^{65}Cu isotopes in their natural abundance. Only the ^{63}Cu hyperfine values are reported in this manuscript because the ^{65}Cu hyperfine values can be easily calculated by multiplication with the ratio of the nuclear g values ($g_n(^{65}Cu)/g_n(^{63}Cu) = 1.07$).

SS-NMR ^{13}C spectra were recorded on a Varian InfinityPlus 400 spectrometer working at ^{1}H and ^{13}C Larmor frequencies of 400.03 and 100.60 MHz, respectively, using a 7.5 mm probehead with ^{1}H and ^{13}C 90° pulse durations of 5 μs. ^{13}C Cross-Polarization Magic Angle Spinning (CP-MAS) spectra were all registered under high power proton decoupling conditions and using the following parameters chosen after suitable calibrations: (a) for PBMA-N3 a MAS frequency of 3 kHz, a contact time of 1 ms, a recycle delay of 2 s and 3200 transients, (b) for Am-PA a MAS frequency of 5.5 kHz, a contact time of 1 ms, a recycle delay of 7 s and 40 transients, (c) for Am-g-PBMA a MAS frequency of 3 kHz, a contact time of 0.5 ms, a recycle delay of 2 s and 21,600 transients. ^{13}C Delayed CP-MAS spectra were recorded with the same parameters used for CP-MAS spectra, inserting a delay of 100 μs between the ^{1}H 90° pulse and the CP pulse (Cudby et al., 1985). ^{13}C Direct-Excitation Magic Angle Spinning (DE-MAS) spectra were all registered using the DEPTH pulse sequence (Cory & Ritchey, 1988) under high power proton decoupling conditions, with a MAS frequency of 3 kHz, a recycle delay of 2 s and accumulating about 2000 transients for each sample. ^{13}C chemical shift scale was referred to hexamethylbenzene and TMS as secondary and primary references, respectively. All the spectra were registered at 20 °C, using air as spinning gas.

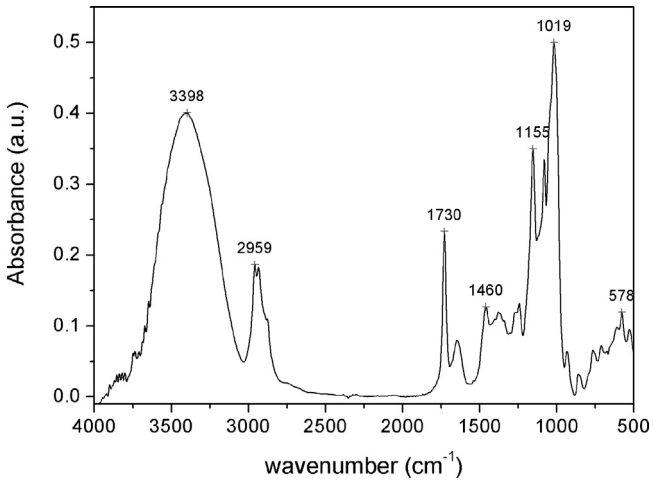

Fig. 1. FT-IR spectrum of Am-g-PBMA on a KBr pelletized dish.

The measurements of proton free induction decays (FID's) and T_1 were carried out on a Varian XL-100 spectrometer coupled with a Stelar PCNMR acquisition system, working at a ^{1}H Larmor frequency of 24.1 MHz, using a ^{1}H 90° pulse duration of 4 μs. Proton FIDs were acquired under on-resonance conditions using a solid echo pulse sequence with an echo delay of 14 μs, a recycle delay of 1 s and accumulating 100 transients. Proton T_1 relaxation times were measured by means of an inversion recovery-solid echo pulse sequence, using a recycle delay of 1 s and accumulating 16 transients. All the measurements were carried out a 20 °C.

3. Results and discussion

3.1. Preparation of the Am-g-PBMA copolymer

The amylose-*graft*-poly(n-butyl methacrylate) copolymer (Am-g-PBMA) was obtained by coupling between alkyne and azide moieties of alkyne-functionalized amylose (Am-PA) and azide-functionalized poly(n-butyl methacrylate) (PBMA-N3), respectively, under Cu(I) catalyzed 1,3-dipolar cycloaddition conditions according to a procedure previously set up in our laboratory (Scheme 1) (Bertoldo et al., 2011).

Am-PA was prepared by functionalization of amylose with alkyne moieties under mild conditions in a two steps procedure consisting in quantitative oxidation with periodate followed by reductive amination with propargyl amine. The achieved functionalization degree, as calculated from the nitrogen content by elemental analysis, was 0.045 mol/mol of glucoside units, in good agreement with previous results (Bertoldo et al., 2011).

PBMA-N3 was obtained by BMA polymerization from the azide functionalized initiator BIAA synthesized *ad hoc* (see Supplementary data). The $\bar{M}_n$ value by SEC analysis was 6.5 kDa, in good agreement with the theoretical value of 6.2 kDa. The presence of the azide functionality in the polymer was confirmed by the stretching band at 2100 cm^{-1} in the infrared spectrum (Fig. S1 of Supplementary data).

Am-PA and PBMA-N3 were finally coupled under click conditions. The success of the reaction was proven by infrared analysis of the product recovered by precipitation in diethyl ether (Fig. 1). The FT-IR spectrum shows absorption bands of both amylose, such as the band at 1019 cm^{-1} associated to the saccharide ring, and PBMA, such as the characteristic band at 1730 cm^{-1} due to the carbonyl group. Am-g-PBMA was purified by double precipitation in

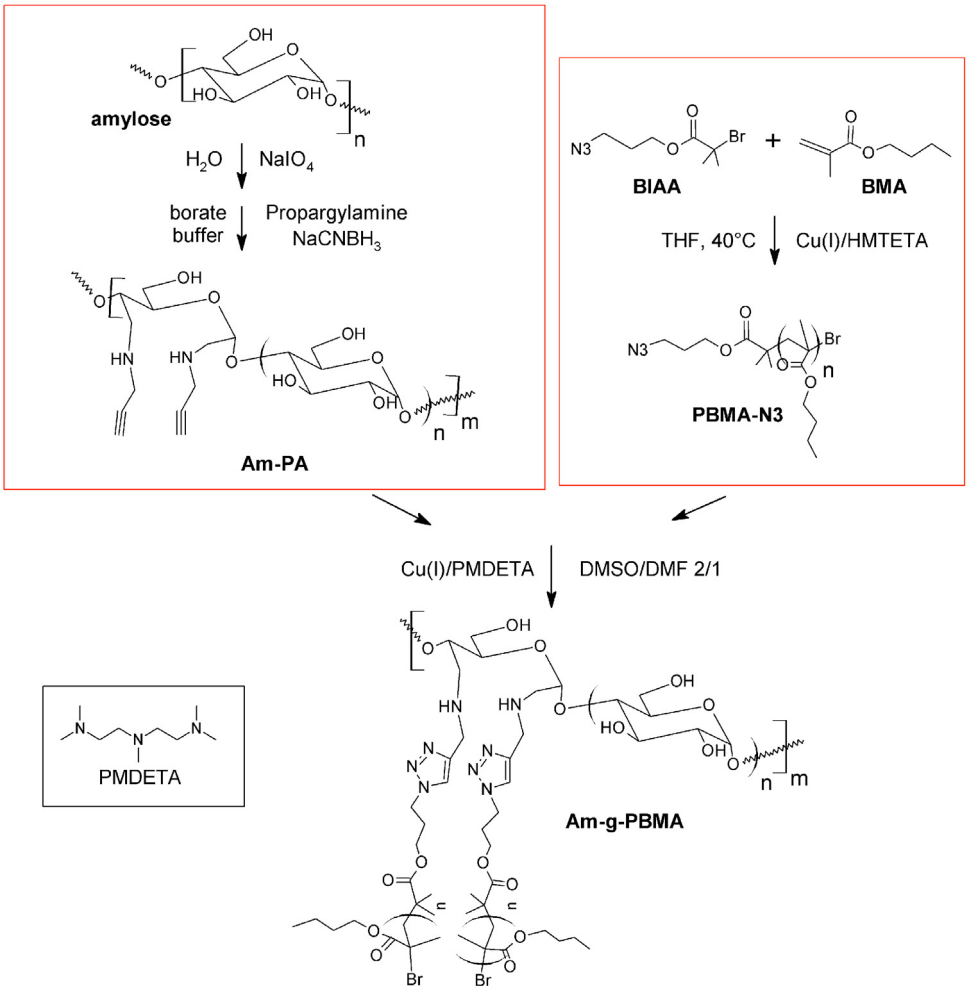

Scheme 1. Preparation of amylose-*graft*-poly(n-butyl methacrylate) (Am-g-PBMA).

diethyl ether to remove any unbounded polymethacrylate and no detectable polymer was observed by infrared spectroscopy in the liquid phase after the second precipitation.

The sample was further purified by solubilization in DMSO (20 g/L), diluted with distilled water (1.5 g/L) and dialyzed versus distilled water for 3 days. The solid sample was recovered by lyophilization. The copolymer composition was determined by TGA analysis, by comparing the weight loss peaks of Am-g-PBMA with those of its constituents, namely Am-PA and PBMA-N3 (Fig. 2). In fact, Am-g-PBMA degraded in two steps: the peak at lower temperature was assigned to both Am-PA and PBMA-N3 and that at higher temperature to the sole PBMA-N3. The weight percentage of PBMA in Am-g-PBMA was then calculated by comparing the high temperature peak in the copolymer and in the pure PBMA-N3; it was found to be 52%.

3.2. Am-g-PBMA morphology

In a previous paper (Bertoldo et al., 2011) the ability of Am-g-PBMA to self-assemble in water forming nanoparticles was proven by dynamic light scattering investigation, as well as by transmission electron microscopy observation. Since the procedure adopted to induce self-assembling was the same here used in the final purification step, it is reasonable to infer that similar self-assembling of Am-g-PBMA occurs also in the present case. As a matter of fact, the dispersion recovered after dialysis was stable, as clearly indicated by its transparent appearance and by the absence of any precipitate. Moreover, further storage in laboratory for at least two months did not evidence any change.

After lyophilization, the recovered copolymer looked like a soft crochet or a sponge dish. The scanning electron microscopy (SEM) analysis showed a complex morphology consisting in spherical particles plunged into a fiber network (Fig. 3), most particles having diameter in the micrometer range. However, at high magnification nanometric particles could be observed on the surface of larger par-

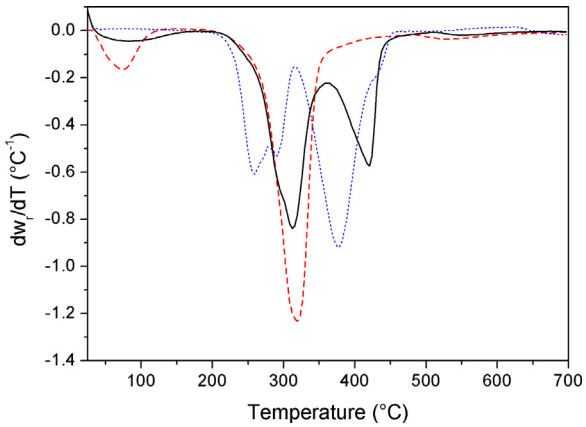

Fig. 2. First derivative plots of the thermogravimetric analyses (DTGA) of Am-g-PBMA (black solid line), Am-PA (red dashed line) and PBMA-N3 (blue dotted line).

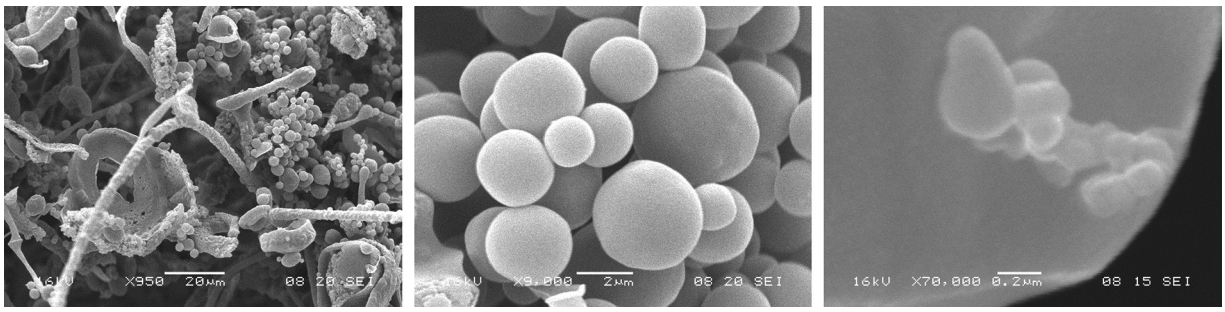

Fig. 3. SEM micrographs of solid Am-g-PBMA obtained by lyophilization of a water dispersion.

ticles and fibers. It can be speculated that the observed morphology results from the aggregation of the nano-sized particles present in the water dispersion.

3.3. Binding of residual Cu(II) by EPR spectroscopy

Although extensive dialysis against water significantly lowered the content of residual copper from the catalyst in the copolymer, it was not completely removed, as already found by other authors after extensive washing with EDTA solutions (Wang et al., 2012). Indeed, the ICP-OES analysis revealed that the residual copper in the copolymer is 1.46 ± 0.05 mg/g before and 422 ± 1 μg/g after the last purification step by dialysis. The last amount corresponds to ~7% of the copper introduced in the reaction with the catalyst. Considering the reaction and purification conditions, the major part of copper should be present in the Am-g-PBMA copolymer as Cu(II), which can be investigated by acquisition and line shape analysis of EPR spectra.

X-band EPR experiments were performed on the solid copolymer at 298 K and at 120 K obtaining spectra with essentially the same features, both reflecting the superposition of two spectral components; the low temperature spectrum is reported in Fig. 4.

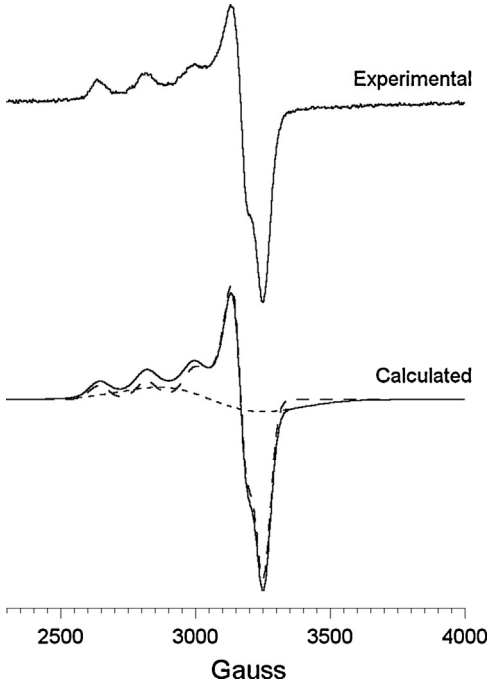

Fig. 4. Experimental (top) and calculated (bottom) X-band EPR spectrum of Am-g-PBMA at 120 K; long-dashed and short-dashed lines represent the calculated spectra of species 1 and 2, respectively.

One spectral component presents features typical of isolated Cu(II) centers with the unpaired electron spin in a $d_{x^2-y^2}$ ground state and a square pyramidal geometry, that is an axial symmetry of the **g** and hyperfine (**A**) tensors, with $g_{||} > g_{\perp} > 2.0023$ (Species 1). The hyperfine structure, due to the coupling of the unpaired electron spin with the Cu nuclear spin (both ^{63}Cu and ^{65}Cu isotopes have spin equal to 3/2), is well resolved in the parallel region. The other subspectrum is instead an unstructured very broad line (Species 2). A fitting of the spectrum allowed the magnetic parameters characterising the two components to be determined together with their relative contribution to the whole spectral intensity; the calculated spectra are shown in Fig. 4 and the corresponding parameters are reported in Table 1.

The $g_{||}$ and $A_{||}$ values determined for the isolated Cu(II) species (Species 1 in Table 1) are similar to those found for complexes of Cu(II) with PMDETA and other ligands in frozen solution (Kroczewska, Bogusz, Kurzak, & Jezierska, 2002; Kurzak, Kamecka, Bogusz, & Jezierska, 2007; Patel, Singh, Gundla, & Chauhan, 2007; Patel et al., 2004), and correspond to the equatorial ligation of 3–4 nitrogen atoms to Cu(II) according to the tables of Peisach and Blumberg (Peisach & Blumberg, 1974). Therefore, the isolated complexes can be envisaged as Cu(II) centers coordinated to the PMDETA nitrogens and to other ligands from the copolymer through nitrogen and/or oxygen atoms. In particular, quite strong complexes could form with triazole nitrogens, although coordination of Cu(II) to amylose OH groups cannot be excluded. In order to better assign this species, EPR spectra were recorded in frozen solution at 120 K on reference samples containing the sole catalyst (CuBr/PMDETA), the catalyst plus amylose, and the catalyst plus PBMA-T (see Scheme 2) and compared with those of solid Am-g-PBMA. The magnetic parameters obtained from the spectral analysis (see Table 1) showed that practically equal $g_{||}$ (g_{zz}) and $A_{||}$ (A_{zz}) parameters are observed for the copolymer and the model sample that contains the catalyst and PBMA-T. This observation suggests that the isolated Cu(II) centers present in the copolymer

Table 1
g and hyperfine (**A**) tensor components used in the fitting of the X-band EPR spectra recorded at 120 K on solid Am-g-PBMA and on frozen DMF/DMSO solutions of reference samples.

Sample	Species 1	Species 2
Am-g-PBMA	$g_{||} = 2.256$; $g_{\perp} = 2.066$ $A_{||} = 174$ G; $A_{\perp} = 11$ G Spectral weight = 65%	$g_{av} = 2.141$ Spectral weight = 35%
CuBr/PMDETA 1/1	$g_{zz} = 2.242$, $g_{xx} = 2.065$, $g_{yy} = 2.056$ $A_{zz} = 167$ G, $A_{xx} = 2$ G, $A_{yy} = 42$ G	
CuBr/PMDETA 1/1 + amylose	$g_{zz} = 2.245$, $g_{xx} = 2.063$, $g_{yy} = 2.056$ $A_{zz} = 163$ G, $A_{xx} = 4$ G, $A_{yy} = 39$ G	
CuBr/PMDETA 1/1 + PBMA-T	$g_{zz} = 2.238$, $g_{xx} = 2.067$, $g_{yy} = 2.054$ $A_{zz} = 173$ G, $A_{xx} = 28$ G, $A_{yy} = 0$ G	

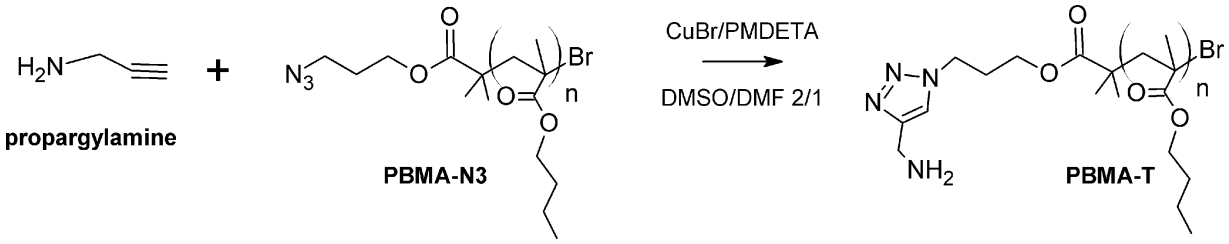

Scheme 2. Synthesis of PBMA-T.

are most probably coordinated to the PMDETA ligand, as in the catalyst, and to a triazole nitrogen. Furthermore, in the copolymer there are neither free Cu(II) species coordinated only to water molecules, nor isolated species with Cu(II) bound only to amylose hydroxyl groups. Indeed, these last species give signals with $g_{||}$ and $A_{||}$ sensibly higher and lower (i.e. $g_{||} \sim 2.442$ and $A_{||} \sim 120$ G as reported by Łabanowska et al. (2006) and Zhang et al. (2010)) with respect to those measured here. Moreover, it must be noticed that a signal characterized by $g_{||} = 2.300$ and $A_{||} = 159$ G, that is values similar to those found for the model sample containing the catalyst and amylose (Table 1), was also present in the EPR spectra acquired on solid Am-g-PBMA before the dialysis purification step (see Fig. S3 in the Supplementary data). This finding, together with data from ICP-OES analysis, indicates that water dispersion and prolonged dialysis were able to remove isolated species of copper coordinated to the PMDETA ligand and bound to amylose chains. On the contrary, residual copper coordinated to the triazole nitrogens is more difficult to be removed.

The broad signal, centered at $g_{av} = 2.141$ and showing a width of ~380 G (Species 2 in Table 1), is characteristic of clustered Cu(II) centers giving strong dipolar interactions among them (Caretti et al., 2010). These centers could belong to poly-nuclear complexes where Cu(II) ions are linked through mutual ligands and/or to Cu(II) complexes spatially confined by trapping into the polymeric matrix. These Cu(II) species, observed in the EPR spectra of Am-g-PBMA both before (Fig. S3 in Supplementary data) and after (Fig. 4) purification, are difficult to be removed too. Considering that Cu(II) ions have been found to induce self-assembly of amylose in aqueous solution (Li et al., 2013, 2014), with Cu(II) coordinated to spatially close hydroxyl groups of amylose, also forming polynuclear complexes, we can ascribe the broad EPR signal to Cu(II) species coordinated to amylose entrapped in the solid copolymer.

3.4. Structural and dynamic properties of Am-g-PBMA by SS-NMR

The ^{13}C Cross Polarization Magic Angle Spinning (CP-MAS) spectra of Am-g-PBMA and of its constituent polymers PBMA-N3 and Am-PA are reported in Fig. 5a. In the spectrum of PBMA-N3 all the inequivalent carbon nuclei of the monomer give rise to a specific signal (with the exception of the two methyl carbons that resonate at approximately the same chemical shift) and the signal assignment is straightforward, based also on literature data (Pascui & Reichert, 2004; Quinting & Cai, 1994). Signals arising from PBMA-N3 chain-ends are not observable due to their too low concentration. Also for Am-PA the assignment of signals in the ^{13}C CP-MAS spectrum is straightforward and reported in Fig. 5a. SS-NMR has been exploited in the study of starches since the beginning of its application and a detailed literature is available on the correlation between ^{13}C CP-MAS spectral features and starch structural features. Amylose is, together with amylopectin, one of the main components of starch and the two macromolecules exhibit similar spectral characteristics. The spectrum of Am-PA shows the peculiar features of a mainly amorphous starch: signals are broad and scarcely resolved, the signal of C1 has components at 103 and 95 ppm and a peak ascribable to C4 is observed at 82 ppm. The spectrum is very similar to those previously reported for amorphous potato starches, in agreement with the origin of the amylose employed for Am-PA preparation, and the substantially amorphous character of the sample as inferred from the spectrum is in agreement with the treatments experienced by amylose to obtain Am-PA (Gidley & Bociek, 1985; Paris, Bizot, Emery, Buzaré, & Buléon, 1999; Veregin, Fyfe, Marchessault, & Taylor, 1986). Signals arising from propargyl groups are not observable in the spectrum of Am-PA due to their low concentration.

The ^{13}C CP-MAS spectrum of the Am-g-PBMA copolymer is substantially the sum of the spectra of PBMA-N3 and Am-PA, only small differences being observed for signal intensities and widths. These findings indicate that no dramatic structural changes occur to either PBMA or amylose upon click reaction and subsequent purification in water and lyophilization. Small but detectable changes can be observed for signals of PBMA, which appear broader than those of pristine PBMA-N3. This effect can be ascribed to an increased structural disorder of PBMA as a consequence of the grafting onto amylose, which brings each carbon to experience a distribution of environments and, as a consequence, of isotropic chemical shifts. Moreover, the intensity of the signals of carbons 4 and 5 seems increased, which could indicate a certain stiffening of the PBMA side chains. It is indeed useful to remind that the intensity of the signals in CP spectra depends on the strength of the ^{1}H–^{13}C dipolar couplings, which in turn is determined not only by the number of protons spatially close to the carbon nucleus considered, but also by the degree of mobility of the local environment. In particular, the intensity of carbon nuclei bound to a higher number of protons in rigid environments is enhanced in ^{13}C CP spectra.

For obtaining complementary information on the dynamic properties of PBMA and amylose in the copolymer we recorded ^{13}C Direct Excitation (DE) MAS spectra using a short recycle delay (2 s) between two consecutive scans (Fig. 5b). This is a common way for obtaining ^{13}C spectra that selectively contain only signals arising from carbon nuclei with a short spin-lattice relaxation time (T_1), such as those of molecular fragments and environments characterized by a high degree of mobility (as far as motions with characteristic frequencies of the order of the Larmor frequency, in this case 100 MHz, are concerned). The selective ^{13}C DE-MAS spectrum of PBMA-N3, compared with the CP-MAS one, shows a strong relative decrease of the intensity of the signals of the main chain carbon nuclei, indicating that these nuclei, opposite to those of the side chain, have a long T_1. This is expected if we consider that, at the analysis temperature, the polymer is below the glass transition temperature T_g, where only the motions of the side chains are active (Pascui & Reichert, 2004). As far as Am-PA is concerned, the comparison of the ^{13}C DE-MAS and CP-MAS spectra indicates that all the signals survive to the T_1 filter, even if they appear strongly decreased in intensity, the C6 signal being now the most intense. This indicates that amylose is substantially rigid with the only exception of the C6–OH group, which experiences a fast

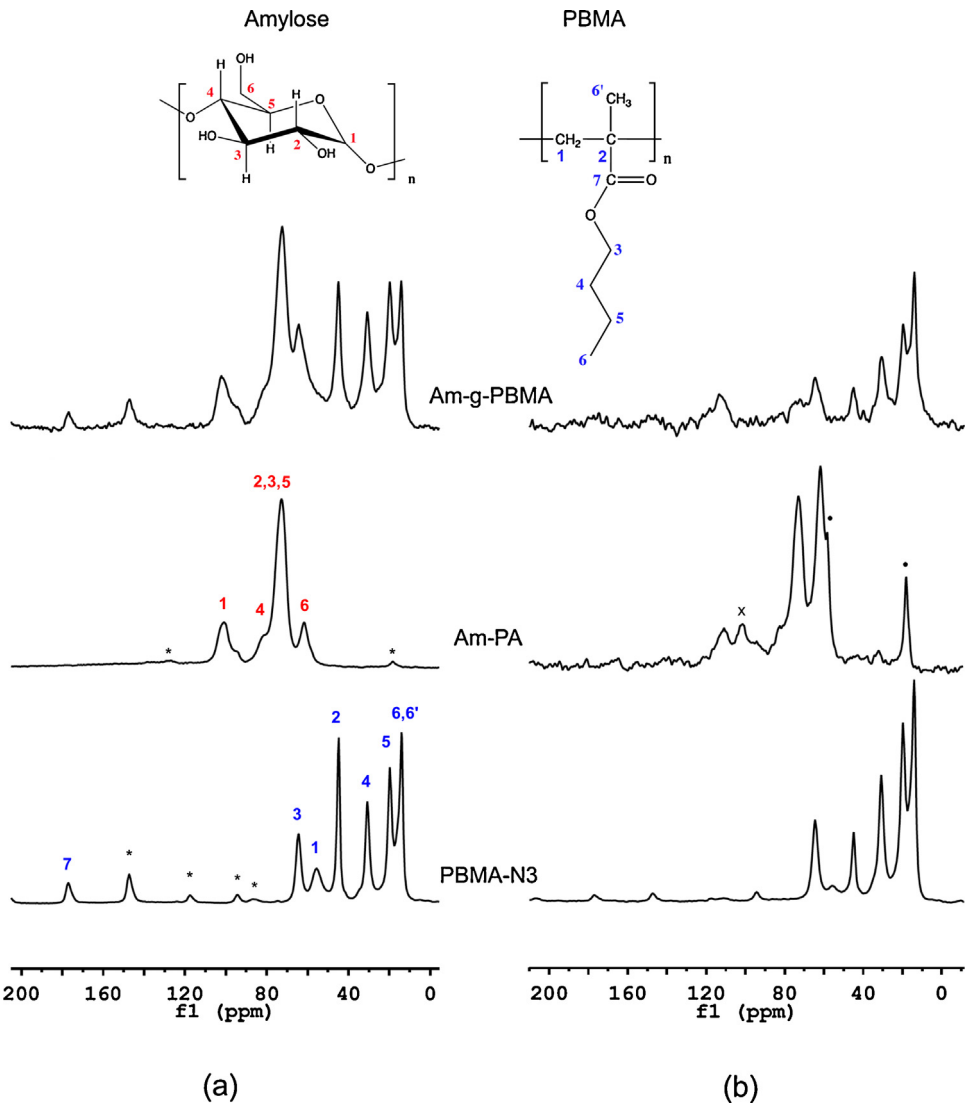

Fig. 5. (a) ^{13}C CP-MAS spectra and (b) ^{13}C DE-MAS spectra recorded with a recycle delay of 2 s on, from top to bottom, Am-g-PBMA, Am-PA and PBMA-N3. Amylose (left) and PBMA (right) structures are reported on the top of the figure with the atom numbering used for spectral assignment. * indicate spinning side bands, × indicates a signal arising from probehead background, ● indicate signals of entrapped ethanol.

inter-conformational motion that shortens its ^{13}C T_1. This result is in agreement with those already reported in the literature for amylose and starch (Horn, Yamamoto, Hirai, & Kitamaru, 1987; Tang & Hills, 2003). It must be mentioned that, in the ^{13}C DE-MAS spectrum of amylose, signals at 18 and 58 ppm must be ascribed to traces of entrapped liquid ethanol, while that at 110 ppm arises from incomplete suppression of the probe background signal. It is interesting to notice that in the ^{13}C DE-MAS spectrum of Am-g-PBMA, while PBMA signals are clearly visible, those of amylose appear almost completely suppressed, indicating an increase of ^{13}C T_1's with respect to pure amylose. This can be interpreted as a stiffening of amylose in passing to the copolymer.

Further complementary dynamic information could be obtained by recording ^{13}C Delayed CP-MAS spectra, in which signals arising from carbon nuclei coupled to protons with quite long transverse relaxation times (T_2) are selectively observed. Proton T_2 increases with increasing molecular mobility in the characteristic frequency range of 1–10 kHz (slow-intermediate motional regime), thus is sensitive to motions slower than those affecting ^{13}C T_1. We recorded ^{13}C Delayed CP-MAS spectra with a delay of 100 μs between the ^{1}H 90° pulse and the contact pulse, and for all samples it was practically impossible to detect any signal, indicating the substantial absence of ^{1}H nuclei with long T_2 coupled to carbon nuclei and, consequently, the lack of corresponding polymer moieties undergoing motions in the slow-intermediate regime.

With the aim of investigating the dynamic properties of the system more in depth, we performed low-resolution experiments for measuring ^{1}H T_2 and T_1. In particular, proton T_2 were obtained by analyzing the proton Free Induction Decays (FIDs) of the samples recorded under on-resonance conditions at low magnetic field (Fig. 6). In these conditions, ^{1}H FIDs can be reproduced with a linear combination of analytical functions, each of them characterized by a T_2 and a weight percentage; the best linear combination is found through a fitting procedure (Borsacchi, Cappellozza, Catalano, Geppi & Ierardi, 2006; Hansen, Kristiansen & Pedersen, 1998). In particular, the best linear combination of functions for fitting each sample FID ($I = f(t)$) was chosen on the basis of the Occam's Razor principle and of the minimization of the sum of the squared residuals χ^2. Functions were chosen among Gaussian

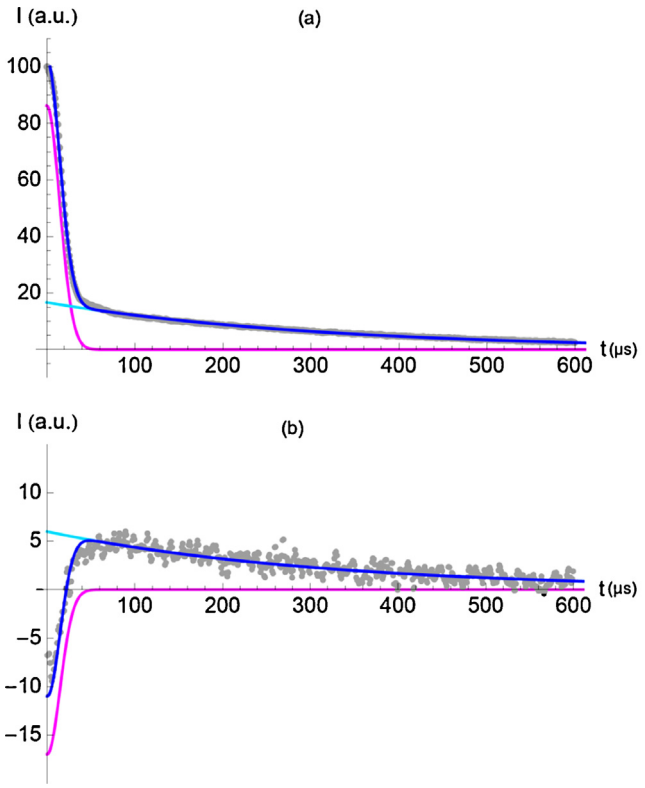

Fig. 6. (a) Analysis of ^{1}H FID of Am-g-PBMA. Experimental FID (gray); best-fitting function (linear combination of Gaussian and exponential functions) (blue); Gaussian (magenta) and exponential (light blue) functions linearly combined in the best-fitting function. (b) Analysis of ^{1}H FID registered at a delay $\tau = 20$ ms of the Inversion Recovery pulse sequence used for measuring ^{1}H T_1.

($I(t) = I(0)e^{-(t/T_2)^2}$), exponential ($I(t) = I(0)e^{-(t/T_2)}$), Weibullian ($I(t) = I(0)e^{-(t/T_2)^n}$, with $1 < n < 2$) and Pake (Eq. (1)).

$$I(t) = \sqrt{\frac{\pi}{6}} e^{-(\beta^2 t^2/2)} \left[\frac{\cos\alpha t}{\sqrt{\alpha t}} C\left(\sqrt{\frac{6\alpha t}{\pi}}\right) + \frac{\sin\alpha t}{\sqrt{\alpha t}} S\left(\sqrt{\frac{6\alpha t}{\pi}}\right) \right] \quad (1)$$

where $\alpha = 3\gamma^2\hbar/4R_{HH}^3$ and R_{HH} is the internuclear distance between the two most strongly dipolarly coupled protons, β is the width of the Gaussian broadening function, which takes into account the dipolar interactions with the other protons, C(x) and S(x) are the Fresnell functions, whose expression can be found in Hansen, Kristiansen, and Pedersen (1998). The obtained results of the FID analysis of PBMA-N3, Am-PA and Am-g-PBMA are reported in Table 2. In solid samples T_2 are usually very short (of the order of 10–100 μs) and, out of the rigid lattice regime (where motions, if present, have characteristic frequencies smaller than the dipolar static interactions and they do not affect T_2), T_2 monotonically increases with increasing mobility.

The ^{1}H FID of PBMA-N3 was well reproduced with the sum of a Gaussian function and an exponential function both characterized by a short T_2, in agreement with the result of ^{13}C Delayed CP-MAS spectrum. This is in accord with the glassy state of the polymer and indicates that the reorientational motions of the side chains do not have the effect of reducing the proton homonuclear couplings (which would determine an increase of T_2), probably for geometrical reasons. The ^{1}H FID recorded for Am-PA was instead reproduced with a combination of a Pake function, representing a fraction of protons with very low mobility, and an exponential function with a long T_2 ascribable to a fraction of more mobile protons. Even if it has been reported that some amorphous starch polysaccharide fractions, especially in hydrated samples, can have a quite long T_2 (Tang & Hills, 2003), in our case the ^{13}C Delayed CP-MAS experiment indicated the absence of ^{1}H nuclei, coupled with ^{13}C nuclei, with long T_2. On the other hand, amylose is hygroscopic and, in equilibrium with atmosphere moisture, has ~ 10 wt% of adsorbed water which can form hydrogen bonds with amylose OH groups. In the investigated sample the water content, determined by TGA analysis, was 7 ± 1 wt%. The water and amylose OH protons can experience a higher mobility and a smaller homonuclear coupling with respect to polysaccharide ring protons, resulting in a longer T_2. Moreover, the dipolar couplings of these protons with carbon nuclei of amylose are reasonably not sufficiently strong to give cross-polarization, thus explaining the absence of signals in the ^{13}C Delayed CP-MAS spectrum of Am-PA. By roughly calculating the relative amounts of CH protons, and OH and water protons, a 62:38 ratio was found. Considering all the experimental errors, these values are in very good agreement with the weights of the Pake and the exponential functions (64% and 36%), even though the very small amount of ethanol present should slightly increase the calculated weight of the exponential function.

Following the criterion of keeping at minimum the number of functions necessary for obtaining a good reproduction of the experimental data, the FID acquired for Am-g-PBMA was reproduced by the sum of two functions: a Gaussian and an exponential (Fig. 6a). The former had a short T_2, very similar to that of the Gaussian function used for PBMA-N3, and the latter had a quite long T_2, similar to that assigned to amylose hydroxyl groups and water protons (Table 2). The weight ratio between the two functions was 84:16 (Table 2) which is very close to the ratio (86:14) between the number of protons found in rigid environments (that is all PBMA-N3 protons and 63.6% of amylose protons) and that of mobile protons of amylose and water. On the other hand the results of the analysis of Am-g-PBMA FID indicate that both a fraction of PBMA-N3 (that with a T_2 of 30.9 μs) and especially amylose and amylose-interacting water experience a certain stiffening in passing to the copolymer. It is worth to notice that a reduction of molecular mobility of amylose and, to a minor extent, of PBMA, was already inferred from ^{13}C spectra.

For further investigating the dynamic properties of this system, as well as obtaining information on the mixing degree of PBMA and amylose in the copolymer, we measured proton T_1's. The results are reported in Table 2. In the solid state, proton spin-lattice relaxation times are strongly affected by the spin-diffusion process that tends to average to the same value different intrinsic T_1's of protons belonging to domains intimately mixed on a 10 nm scale. Therefore, in this case we measured ^{1}H T_1 of PBMA-N3 and Am-PA,

Table 2
Results of ^{1}H FID analysis and T_1 measurements at a Larmor frequency of 24 MHz and a temperature of 20 °C. For each sample the functions used for reproducing the FID (g: Gaussian, e: exponential, p: Pake) with their T_2 and weight percentage are reported; uncertainties on the reported values are less than 1%. For obtaining PBMA-N3 and Am-PA T_1's the magnetization recovery curves were fitted with a mono-exponential function, while in the case of Am-g-PBMA a bi-exponential function was necessary.

Sample	f_a	T_{2a} (μs)	w_a%	f_b	T_{2b} (μs)	w_b%	T_1 (ms)	w%
PBMA-N3	g	20.1	78.0	e	30.9	22.0	98 ± 3	100
Am-PA	p	[a] $T_2 = 43.3R_{HH} = 1.954$ Å$\beta = 32627$ Hz	63.6	e	479	36.4	85 ± 2	100
Am-g-PBMA	g	20.8	83.8	e	315.2	16.2	7 ± 155 ± 3	36 ± 364 ± 3

[a] T_2 can be calculated as $\sqrt{2}/\beta$.

with the aim of comparing them with those of the copolymer. As it is possible to see in Table 2 both reactants showed a single T_1 value, indicating that, as expected in the case of pure compounds, both polymers are homogeneous on a 10 nm scale. Unfortunately the T_1 values measured for PBMA-N3 and Am-PA resulted to be very similar, thus preventing the T_1 measured for the Am-g-PBMA copolymer from being a useful probe for the mixing degree of the two polymers. On the other hand, the measurement of T_1 of Am-g-PBMA protons could be of help in unravelling the location of Cu(II) in the copolymer. Indeed the fitting of the magnetization recovery curve of Am-g-PBMA required two different T_1's, one of which extremely short (7 ms). Such a short T_1 cannot be justified on the basis of dynamic properties and must be due to the presence of paramagnetic species identifiable with Cu(II) arising from the catalyst. Indeed Cu(II) centers are known to determine strong T_1 shortening for nuclei at distances up to several Angstroms (and the effect can be then transferred farer through spin-diffusion for protons), while having negligible effect on T_2 relaxation (indeed we did not observe any particularly short T_2 component in the ^{1}H FID of the copolymer) (Nadaud, Helmus, Kall, & Jaroniec, 2009). Due to the mixing effect of spin-diffusion, proton T_1 data by themselves cannot give information on which protons are likely to be close to Cu(II) centers. On the other hand a useful indication came from the analysis of the evolution of the ^{1}H FID shape during the inversion-recovery experiment used for measuring T_1. This is exemplified in Fig. 6b that shows the analysis of the ^{1}H FID registered at a value of 20 ms of the variable delay of the Inversion Recovery experiment used for measuring ^{1}H T_1. At this value of the delay it is clear that the magnetization recovery driven by the spin-lattice relaxation (T_1) for the exponential function (the intensity of which is here positive) is remarkably faster than that of the Gaussian function (the intensity of which is still negative). Therefore, it is possible to state that the FID component most strongly associated with the shortest T_1 is that with the longest T_2. This observation suggests that the NMR detectable Cu(II) species could be mainly located quite close to amylose OH groups and adsorbed water.

Considering the results of the EPR investigation and that Cu(II) ions have been found to induce self-assembly of amylose in aqueous solution (Li et al., 2013, 2014), we can infer that the Cu(II) coordinated to amylose hydroxyls could be the multi-nuclear or clustered Cu(II) species detected by EPR in solid Am-g-PBMA (species 2 in Table 1).

4. Conclusions

The Am-g-PBMA copolymer was successfully prepared following a procedure based on click chemistry. Although extensive dialysis against water significantly lowered the content of residual copper from the catalyst in the copolymer, it was not completely removed. In particular, EPR spectroscopy indicated that complexes of Cu(II) coordinated to the PMDETA ligand from the catalyst and to the copolymer triazole nitrogens were not removed. Further residual copper was found to be present as multi-nuclear or clustered Cu(II) species likely coordinated to amylose hydroxyl groups. Moreover, a combined ^{1}H and ^{13}C SS-NMR investigation of the Am-g-PBMA copolymer and of starting Am-PA and PBMA-N3 polymers showed that copolymerization and self-assembly in water bring to a considerable stiffening of the amylose chains and an increased structural disorder of PBMA chains.

Acknowledgements

This research was funded by the National Project "New Polymer Systems with Electric and Optical Functionalities via Nano and Micro Adhesive Dispersion to Produce Materials and Devices for Smart Applications" POLOPTEL 2011–2014, La Fondazione CARIPISA conv. 167/09.

Marco Carlo Mascherpa is kindly acknowledged for performing ICP-OES analyses.

Appendix A. Supplementary data

Supplementary data associated with this article can be found, in the online version, at http://dx.doi.org/10.1016/j.carbpol.2014.05.086.

References

Adhikary, P., & Krishnamoorthi, S. (2012). Synthesis, characterization, and application of amylopectin-graft-poly(AM-co-AMPS). *Journal of Applied Polymer Science*, *126*(S1), E313–E318.

Alias, J., Goñi, I., & Gurruchaga, M. (2007). Enzymatic and anaerobic degradation of amylose based acrylic copolymers, for use as matrices for drug release. *Polymer Degradation and Stability*, *92*(4), 658–666.

Beiner, M., & Huth, H. (2003). Nanophase separation and hindered glass transition in side-chain polymers. *Nature Materials*, *2*(9), 595–599.

Bertoldo, M., Zampano, G., La Terra, F., Villari, V., & Castelvetro, V. (2011). Amphiphilic amylose-g-poly(meth)acrylate copolymers through "click" onto grafting method. *Biomacromolecules*, *12*(2), 388–398.

Borsacchi, S., Cappellozza, S., Catalano, D., Geppi, M., & Ierardi, V. (2006). Solid State NMR investigation of the molecular dynamics of cocoon silks produced by different Bombyx mori (Lepidoptera) strains. *Biomacromolecules*, *7*(4), 1266–1273.

Caretti, I., Dervaux, B., Du Prez, F. E., & Van Doorslaer, S. (2010). The nature of Cu (II) species in ATRP: New insights via EPR. *Journal of Polymer Science Part A: Polymer Chemistry*, *48*(7), 1493–1501.

Ciardelli, F., & Penczek, S. (2004). *Modification and blending of synthetic and natural macromolecules: Proceedings of the NATO Advanced Study Institute on modification and blending of synthetic and natural macromolecules for preparing multiphase structure and functional materials*, 6–16 October 2003, Pisa, Italy. Dordeecht: Kluwer Academic Publishers.

Ciesielski, W., & Tomasik, P. (2004). Complexes of amylose and amylopectins with multivalent metal salts. *Journal of Inorganic Biochemistry*, *98*(12), 2039–2051.

Cory, D. G., & Ritchey, W. M. (1988). Suppression of signals from the probe in Bloch decay spectra. *Journal of Magnetic Resonance (1969)*, *80*(1), 128–132.

Crini, G. (2005). Recent developments in polysaccharide-based materials used as adsorbents in wastewater treatment. *Progress in Polymer Science*, *30*(1), 38–70.

Cudby, M. E. A., Harris, R. K., Metcalfe, K., Packer, K. J., Smith, P. W. R., & Bunn, A. (1985). ^{13}C and ^{1}H n.m.r. studies of solid polyolefines. *Polymer*, *26*(2), 169–176.

Elchinger, P.-H., Faugeras, P.-A., Boëns, B., Brouillette, F., Montplaisir, D., Zerrouki, R., et al. (2011). Polysaccharides: The "click" chemistry impact. *Polymers*, *3*(4), 1607–1651.

Feng, C., Li, Y., Yang, D., Hu, J., Zhang, X., & Huang, X. (2011). Well-defined graft copolymers: From controlled synthesis to multipurpose applications. *Chemical Society Reviews*, *40*(3), 1282–1295.

Geppi, M., Borsacchi, S., Mollica, G., & Veracini, C. A. (2009). Applications of solid-state NMR to the study of organic/inorganic multicomponent materials. *Applied Spectroscopy Reviews*, *44*(1), 1–89.

Geppi, M., Mollica, G., Borsacchi, S., & Veracini, C. A. (2008). Solid-state NMR studies of pharmaceutical systems. *Applied Spectroscopy Reviews*, *43*(3), 202–302.

Gidley, M. J., & Bociek, S. M. (1985). Molecular organization in starches: A ^{13}C CP/MAS NMR study. *Journal of the American Chemical Society*, *107*(24), 7040–7044.

Goñi, I., Gurruchaga, M., Valero, M., & Guzman, G. M. (1983). Graft polymerization of acrylic monomers onto starch fractions. I. Effect of the reaction time on grafting methyl methacrylate onto amylose. *Journal of Polymer Science. Part A-1, Polymer Chemistry*, *21*(8), 2573–2580.

Goñi, I., Gurruchaga, M., Vázquez, B., Valero, M., Guzmán, G. M., & Román, J. S. (1994). Graft copolymerization of ethyl acrylate with alkyl methacrylates onto amylose initiated by cerium (IV). Microstructure of graft copolymers with respect to statistical copolymers. *Polymer*, *35*(7), 1535–1541.

Hadjichristidis, N., Pispas, S., Pitsikalis, M., Iatrou, H., & Lohse, D. (2004). Graft copolymers. In *Encyclopedia of polymer science and technology*. New York: John Wiley & Sons, Inc.

Hansen, E. W., Kristiansen, P. E., & Pedersen, B. (1998). Crystallinity of polyethylene derived from solid-state proton NMR free induction decay. *Journal of Physical Chemistry B*, *102*(28), 5444–5450.

Horn, F., Yamamoto, H., Hirai, A., & Kitamaru, R. (1987). Structural study of amylose polymorphs by cross-polarization-magic-angle spinning, ^{13}C-N.M.R. spectroscopy. *Carbohydrate Research*, *160*(0), 29–40.

Kalia, S., & Sabaa, W. (2013). *Polysaccharide based graft copolymers*. Barlin Heidelberg: Springer-Verlag.

Karmakar, G. P., & Singh, R. P. (1997). In Anon (Ed.), *Synthesis and characterization of starch-g-acrylamide copolymers for improved oil recovery operations* (pp. 739–745). Houston, TX, USA: Society of Petroleum Engineers (SPE).

Kroczewska, D., Bogusz, K., Kurzak, B., & Jezierska, J. (2002). Potentiometric and spectroscopic study of mixed-ligand copper (II) complexes with N,N,N′,N″,N″-pentamethyldiethylenetriamine and α-(or β-) alaninehydroxamic acids in water solution. *Polyhedron*, *21*(3), 295–303.

Kulbokaite, R., Ciuta, G., Netopilik, M., & Makuska, R. (2009). N-PEG'ylation of chitosan via "click chemistry" reactions. *Reactive and Functional Polymers*, *69*(10), 771–778.

Kurzak, B., Kamecka, A., Bogusz, K., & Jezierska, J. (2007). Unexpected formation of the copper (II) dinuclear mixed-ligand species in the ternary system of N,N,N′,N″,N″-pentamethyldiethylenetriamine with methionine- or histidinehydroxamic acids in aqueous solution. *Polyhedron*, *26*(15), 4345–4353.

Łabanowska, M., Bidzińska, E., Dyrek, K., & Szymońska, J. (2006). Electron paramagnetic resonance study of water distribution in starch granules. *Biopolymers*, *82*(6), 549–557.

Li, Y., Hu, J., Liu, G., Zhang, G., Zou, H., & Shi, J. (2013). Amylose-directed synthesis of CuS composite nanowires and microspheres. *Carbohydrate Polymers*, *92*(1), 555–563.

Li, Y., Lin, S., Hu, J., Liu, G., Zhang, G., Tu, Y., et al. (2014). Metal ion induced-assembly of amylose in aqueous solution. *Carbohydrate Polymers*, *102*, 489–496.

Liu, Z., Jiao, Y., Wang, Y., Zhou, C., & Zhang, Z. (2008). Polysaccharides-based nanoparticles as drug delivery systems. *Advanced Drug Delivery Reviews*, *60*(15), 1650–1662.

Maiti, S., Ranjit, S., & Sa, B. (2010). Polysaccharide-based graft copolymers in controlled drug delivery. *International Journal of PharmTech Research*, *2*(2), 1350–1358.

Mataz, A., & Gregory, B. M. (2005). Effects of confinement on material behaviour at the nanometre size scale. *Journal of Physics: Condensed Matter*, *17*(15), R461.

Matyjaszewski, K., Gnanou, Y., & Leibler, L. (2007). *Macromolecular engineering: Precise synthesis, materials properties, applications*. Weinheim: Wiley-VCH.

Matyjaszewski, K., & Spanswick, J. (2005). Controlled/living radical polymerization. *Materials Today*, *8*(3), 26–33.

Matyjaszewski, K., & Tsarevsky, N. V. (2009). Nanostructured functional materials prepared by atom transfer radical polymerization. *Nature Chemistry*, *1*(4), 276–288.

Matyjaszewski, K., & Xia, J. (2001). Atom transfer radical polymerization. *Chemical Reviews*, *101*(9), 2921–2990.

Matyjaszewski, K. (2012). Atom transfer radical polymerization (ATRP): current status and future perspectives. *Macromolecules*, *45*(10), 4015–4039.

Mooney, B. P. (2009). The second green revolution? Production of plant-based biodegradable plastics. *Biochemical Journal*, *418*(2), 219–232.

Nadaud, P. S., Helmus, J. J., Kall, S. L., & Jaroniec, C. P. (2009). Paramagnetic ions enable tuning of nuclear relaxation rates and provide long-range structural restraints in Solid-State NMR of proteins. *Journal of the American Chemical Society*, *131*(23), 8108–8120.

Nafchi, A. M., Moradpour, M., Saeidi, M., & Alias, A. K. (2013). Thermoplastic starches: Properties, challenges, and prospects. *Starch/Staerke*, *65*(1–2), 61–72.

Nakagawa, A., Kamitakahara, H., & Takano, T. (2012). Synthesis and thermoreversible gelation of diblock methylcellulose analogues via Huisgen 1,3-dipolar cycloaddition. *Cellulose*, *19*(4), 1315–1326.

Nilges, M. (1998). *SIMPIP*. University of Illinois.

Ouhib, R., Renault, B., Mouaziz, H., Nouvel, C., Dellacherie, E., & Six, J.-L. (2009). Biodegradable amylose-g-PLA glycopolymers from renewable resources. *Carbohydrate Polymers*, *77*(1), 32–40.

Paris, M., Bizot, H., Emery, J., Buzaré, J. Y., & Buléon, A. (1999). Crystallinity and structuring role of water in native and recrystallized starches by ^{13}C CP-MAS NMR spectroscopy. 1: Spectral decomposition. *Carbohydrate Polymers*, *39*(4), 327–339.

Pascual, B., Castellano, I., Vazquez, B., Gurruchaga, M., & Goñi, I. (1996). Hydrogels based on graft copolymerization of 2-hydroxypropyl methacrylate/acrylate mixtures on amylose: Swelling behaviour. *Polymer*, *37*(6), 1005–1011.

Pascui, O. F., & Reichert, D. (2004). Influence of side-chain length on main- and side-chain dynamics in poly-n-acrylates: A solid-state NMR study. *Applied Magnetic Resonance*, *27*(3–4), 419–433.

Patel, R., Singh, N., Gundla, V., & Chauhan, U. (2007). Copper (II) complexes of tridentate N,N,N′,N′,N″-pentamethyldiethylenetriamine: Superoxide dismutase and inhibitory activity against bacteria and fungi. *Spectrochimica Acta Part A: Molecular and Biomolecular Spectroscopy*, *66*(3), 726–731.

Patel, R., Singh, N., Shukla, K., Chauhan, U., Niclos-Gutierrez, J., & Castineiras, A. (2004). Magnetic, spectroscopic, structural and biological properties of mixed-ligand complexes of copper (II) with N,N,N′,N′,N″-pentamethyldiethylenetriamine and polypyridine ligands. *Inorganica Chimica Acta*, *357*(9), 2469–2476.

Peisach, J., & Blumberg, W. (1974). Structural implications derived from the analysis of electron paramagnetic resonance spectra of natural and artificial copper proteins. *Archives of Biochemistry and Biophysics*, *165*(2), 691–708.

Peng, P., Cao, X., Peng, F., Bian, J., Xu, F., & Sun, R. (2012). Binding cellulose and chitosan via click chemistry: Synthesis, characterization, and formation of some hollow tubes. *Journal of Polymer Science Part A: Polymer Chemistry*, *50*(24), 5201–5210.

Quinting, G. R., & Cai, R. (1994). High-resolution NMR analysis of the tacticity of poly(n-butyl methacrylate). *Macromolecules*, *27*(22), 6301–6306.

Rostovtsev, V. V., Green, L. G., Fokin, V. V., & Sharpless, K. B. (2002). A stepwise Huisgen cycloaddition process: Copper (I)-catalyzed regioselective "ligation" of azides and terminal alkynes. *Angewandte Chemie*, *114*(14), 2708–2711.

Shogren, R. I., Thompson, A. R., Felker, F. C., Harry-O'Kuru, R. E., Gordon, S. H., Greene, R. V., et al. (1992). Polymer compatibility and biodegradation of starch-poly(ethylene-co-acrylic acid)-polyethylene blends. *Journal of Applied Polymer Science*, *44*(11), 1971–1978.

Silva, I., Gurruchaga, M., & Goñi, I. (2009). Physical blends of starch graft copolymers as matrices for colon targeting drug delivery systems. *Carbohydrate Polymers*, *76*(4), 593–601.

Singh, R. P., Karmakar, G., Rath, S., Karmakar, N., Pandey, S., Tripathy, T., et al. (2000). Biodegradable drag reducing agents and flocculants based on polysaccharides: Materials and applications. *Polymer Engineering & Science*, *40*(1), 46–60.

Singh, R. P., Pal, S., Krishnamoorthy, S., Adhikary, P., & Ali, S. A. (2009). High-technology materials based on modified polysaccharides. *Pure and Applied Chemistry*, *81*(3), 525–547.

Stumpf, W., Conn, P. M., & Preiss, J. (1988). *The biochemistry of plants: Carbohydrates*. Access Online via Elsevier.

Sumerlin, B. S., Tsarevsky, N. V., Louche, G., Lee, R. Y., & Matyjaszewski, K. (2005). Highly efficient "click" functionalization of poly (3-azidopropyl methacrylate) prepared by ATRP. *Macromolecules*, *38*(18), 7540–7545.

Tang, H., & Hills, B. P. (2003). Use of ^{13}C MAS NMR to study domain structure and dynamics of polysaccharides in the native starch granules. *Biomacromolecules*, *4*(5), 1269–1276.

Thirumurugan, P., Matosiuk, D., & Jozwiak, K. (2013). Click chemistry for drug development and diverse chemical-biology applications. *Chemical Reviews*, *113*(7), 4905–4979.

Uliniuc, A., Popa, M., Drockenmuller, E., Boisson, F., Leonard, D., & Hamaide, T. (2013). Toward tunable amphiphilic copolymers via CuAAC click chemistry of oligocaprolactones onto starch backbone. *Carbohydrate Polymers*, *96*(1), 259–269.

Vazquez, M. B., Goni, I., Gurruchaga, M., Valero, M., & Guzman, G. M. (1987). Study of the ceric ion behavior on the inititaion of butyl acrylate polymerization onto amylose. *Journal of Polymer Science, Part A: Polymer Chemistry*, *25*(5), 1309–1314.

Veregin, R. P., Fyfe, C. A., Marchessault, R. H., & Taylor, M. G. (1986). Characterization of the crystalline A and B starch polymorphs and investigation of starch crystallization by high-resolution ^{13}C CP/MAS NMR. *Macromolecules*, *19*(4), 1030–1034.

Vogt, A. P., & Sumerlin, B. S. (2006). An efficient route to macromonomers via ATRP and click chemistry. *Macromolecules*, *39*(16), 5286–5292.

Wang, D. K., Rasoul, F., Hill, D. J. T., Hanson, G. R., Noble, C. J., & Whittaker, A. K. (2012). The role of residual Cu(II) from click-chemistry in the catalyzed hydrolysis of Boltorn polyester-based hydrogels. *Soft Matter*, *8*(2), 435.

Xu, Y., Zhang, Y., & Feng, Q. (2013). The dynamic adsorption performance of the cross-linked starch/acrylonitrile graft copolymer for copper ions in water. *Colloids and Surfaces A: Physicochemical and Engineering Aspects*, *430*, 8–12.

Zhang, J., Junk, M. J., Luo, J., Hinderberger, D., & Zhu, X. (2010). 1,2,3-Triazole-containing molecular pockets derived from cholic acid: The Influence of structure on host–guest coordination properties. *Langmuir*, *26*(16), 13415–13421.

Zhang, Z., Chen, P., Du, X., Xue, Z., Chen, S., & Yang, B. (2014). Effects of amylose content on property and microstructure of starch-graft-sodium acrylate copolymers. *Carbohydrate Polymers*, *102*, 453–459.